Contribution from the Departamento de Quimica Inorgânica, Universidad de Valencia, 46100 Burjassot, Valencia, Spain, Instituto de Ciencia de Materiales de Aragón, Universidad de Zaragoza, CSIC, 50009 Zaragoza, Spain, and Dipartimento di Chimica, Università di Firenze, 50144 Firenze, Italy

Magnetic Interactions and Single-Ion Zero-Field-Splitting Effects in the Two-Sublattice Manganese Chain $MnMn(EDTA)\cdot 9H_2O$: Magnetism and Single-Crystal EPR Spectra

J. J. Borrás-Almenar,[†] R. Burriel,[‡] E. Coronado,*[,†] D. Gatteschi,*[,§] C. J. Gómez-Garcia,[†] and C. Zanchini[§]

Received May 7, 1990

We report on the magnetic susceptibility data and single-crystal EPR spectra of the two-sublattice chain complex $MnMn(EDTA)\cdot 9H_2O$. Its structure consists of infinite zigzag chains parallel to the *a* axis of the orthorhombic cell with alternating hexa- and heptacoordinated metal sites bridged by carboxylate groups: $...Mn(H_2O)_4O_2–Mn(EDTA)(H_2O)–Mn(H_2O)_4O_2...$. The magnetic susceptibility data measured in the 1.1–300 K temperature range show a maximum at about 3 K, which agrees with the presence of an antiferromagnetic intrachain interaction ($J = -0.5$ cm^{-1}), and a sharp peak at $T_c = 1.489$ (2) K, which indicates that the material is a weak ferromagnet in the ordered state. An analysis of the EPR spectra indicates that dipolar interactions between the paramagnetic centers cannot explain the broadening of the lines. A broadening mechanism arising from manganese zero-field splitting is suggested.

Introduction

The bimetallic compounds of the EDTA family formulated as $MM'(EDTA)\cdot nH_2O$, where M and M′ refer to divalent transition-metal ions, have proved to be extremely versatile magnetic materials for the investigation of low-dimensional ferrimagnetic systems.[1] Thus, in the hexahydrate series ($n = 6$) many different metals can easily be accommodated in a chain formed by two alternating different sites, with the consequent control in the size of the spins and the anisotropy of the exchange interaction.[2-5] By conducting the synthesis under conditions of high temperature and pressure, we can obtain the dihydrate series ($n = 2$), in which the elimination of some water results in an intercrossing of the chains and, consequently, in an increase of the dimensionality of the system.[6] The magnetochemistry of these series has been widely investigated by means of specific heat and susceptibility measurements, which has led to information about the strength, nature (isotropic or anisotropic), and dimensionality of the magnetic exchange interactions.

As a part of our studies on low-dimensional ferrimagnets, we have examined the magnetism and single-crystal EPR spectra of the two-sublattice homometallic chain $MnMn(EDTA)\cdot 9H_2O$ in order to obtain information on magnetic interactions and spin dynamics. Its structure has been reported elsewhere[7] and consists of infinite zigzag chains parallel to the *a* axis of the orthorhombic cell with alternating Mn(II) coordination sites. One manganese ion, indicated as [Mn1], is hexacoordinated to four water molecules and to two oxygen atoms of the EDTA ligands, while the other, [Mn2], is heptacoordinated to four oxygen atoms and two nitrogen atoms belonging to the EDTA ligands and one water molecule (Figure 1). On the other hand, slightly alternating Mn1–Mn2 distances occur along the chain, related to different bridging carboxylate topologies. Accordingly, the chain may be schematized as

$$...Mn(H_2O)_4O_2–Mn(EDTA)(H_2O)–Mn(H_2O)_4O_2...$$

Experimental Section

Susceptibility measurements were performed in the temperature range 1.1–300 K with two different techniques. The low-temperature data were obtained in a differential susceptibility setup, at zero static field, with an ac field smaller than 1 Oe at 200 Hz.[8] In these measurements each point is calibrated against cerium magnesium nitrate. The data above 4 K were collected by using a pendulum-type Faraday balance. Single-crystal EPR spectra were recorded at X- and Q-band frequencies with a Varian E9 spectrometer. In the X-band experiment the crystal was rotated by means of a goniometer and a quartz rod, while at Q-band frequency the magnet was rotated. Low-temperature spectra were obtained only at X-band, by use of an Oxford Instruments ESR9 continuous-flow cryostat.

Results and Discussion

Magnetic Properties. The magnetic behavior is reported through a plot of χ_m as a function of temperature in Figure 2, where χ_m is the powder susceptibility per mole. The main features to be noted are as follows: (i) a rounded maximum of χ_m centered at 3 K, which agrees with the presence of short-range antiferromagnetic interactions between manganese ions; (ii) a small and sharp peak that defines a transition to a long-range magnetic ordering at a critical temperature $T_c = 1.489$ (2) K (Figure 3); (iii) a change of slope of the susceptibility curve with a maximum slope at the same critical temperature.

Owing to the large spin of Mn(II), the data in the low-dimensional regime may be fit with the expression calculated by Fisher for a classical-spin Heisenberg chain,[3,9] scaled to a real spin $S = {}^5/_2$:

$$\chi_m = [2Ng^2\mu_B{}^2S(S+1)/3kT](1-u)/(1+u) \qquad (1)$$

where $u = -\coth K + 1/K$, $K = JS(S+1)/kT$, and the exchange Hamiltonian is written as $-JS_iS_j$.

A very close agreement with experiment is obtained with $J = -0.50$ cm^{-1} and $g = 2.0$ (solid line of Figure 2). Despite the weakness of the exchange, the fact that the magnetic data can be described without considering other factors as the alternation in the exchange due to alternating metallic distances, or the local anisotropies of Mn(II), suggests that their effects are too slight to be detectable over the reported temperature range.

Dealing with the nature of the ordered state, it must be noticed that at T_c a small out-of-phase signal is observed in the zero-field susceptibility (Figure 3), which together with the peak indicates

[†] Universidad de Valencia.
[‡] Universidad de Zaragoza, CSIC.
[§] Università di Firenze.

(1) Landee, C. P. In *Organic and Inorganic Low Dimensional Crystalline Materials*; Delhaes, P., Drillon, M., Eds.; NATO-ASI Series B168; Plenum Press: New York, 1987.
(2) Coronado, E.; Drillon, M.; Fuertes, A.; Beltrán, D.; Mosset, A.; Galy, J. *J. Am. Chem. Soc.* **1986**, *108*, 900.
(3) Drillon, M.; Coronado, E.; Beltrán, D.; Georges, R. *Chem. Phys.* **1983**, *79*, 449.
(4) Coronado, E.; Drillon, M.; Nugteren, P. R.; De Jongh, L. J.; Beltrán, D. *J. Am. Chem. Soc.* **1988**, *110*, 3907.
(5) Coronado, E.; Drillon, M.; Nugteren, P. R.; De Jongh, L. J.; Beltrán, D.; Georges, R. *J. Am. Chem. Soc.* **1989**, *111*, 3874 and references therein.
(6) Gómez-Romero, P.; Jameson, G. B.; Casañ-Pastor, N.; Coronado, E.; Beltrán, D. *Inorg. Chem.* **1986**, *25*, 3171. Coronado, E.; Sapiña, F.; Gómez, P.; Beltrán, D.; Burriel, R.; Carlin, R. L. *J. Phys. (Paris)* **1988**, *49*, 853. Coronado, E.; Sapiña, F.; Beltrán, D.; Burriel, R.; Carlin, R. L. *Mol. Cryst. Liq. Cryst.* **1989**, *176*, 507.
(7) Solans, X.; Gali, S.; Font-Altaba, M.; Oliva, J.; Herrera, J. *Afinidad* **1989**, *45*, 243.
(8) Van der Bilt, A.; Joung, K. O.; Carlin, R. L.; De Jongh, L. J. *Phys. Rev. B* **1980**, *22*, 1259.
(9) Fisher, M. E. *Am. J. Phys.* **1964**, *32*, 343.

0020-1669/91/1330-0947$02.50/0

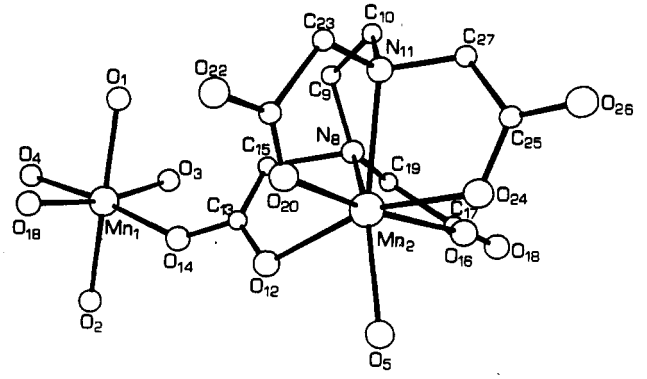

Figure 1. ORTEP view of $MnMn(EDTA)\cdot 9H_2O$ showing the two Mn sites: hydrated [Mn1] and chelated [Mn2].

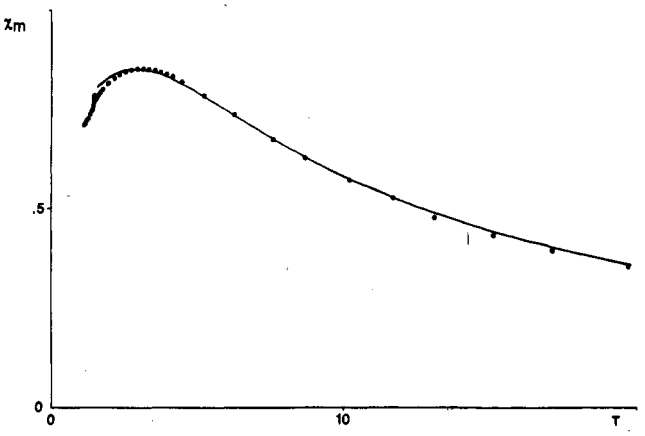

Figure 2. Magnetic behavior of $MnMn(EDTA)\cdot 9H_2O$. The solid line corresponds to the best fit with the Heisenberg classical-spin chain model ($J = -0.50$ cm^{-1}, $g = 2.0$).

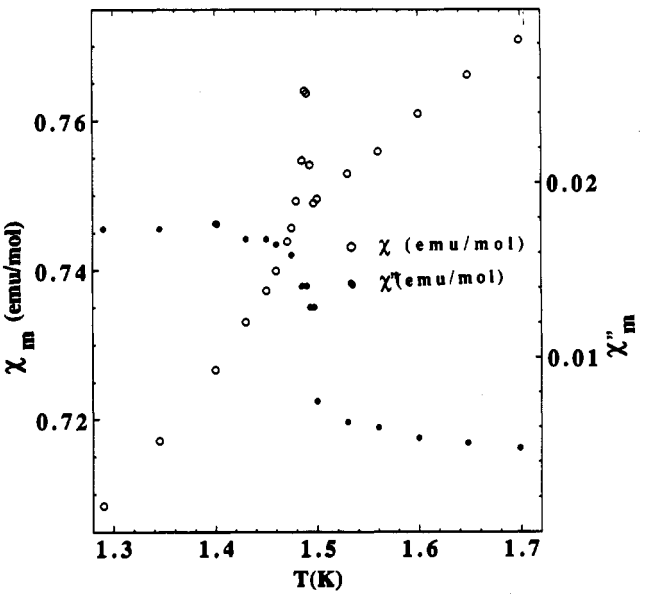

Figure 3. Low-temperature magnetic behavior of $MnMn(EDTA)\cdot 9H_2O$ showing a sharp peak at $T_c = 1.489$ K and an out-of-phase susceptibility (χ_m'') step at the same temperature.

that the material is a weak ferromagnet in the ordered state. The origin of this ferromagnetism may be due to spin canting, since the two octahedral sublattices are alternatingly canted, and furthermore they have different anisotropies (see the next section). We would be able to give an estimation of the canting angle if we had magnetization measurements.[10] From just the complex

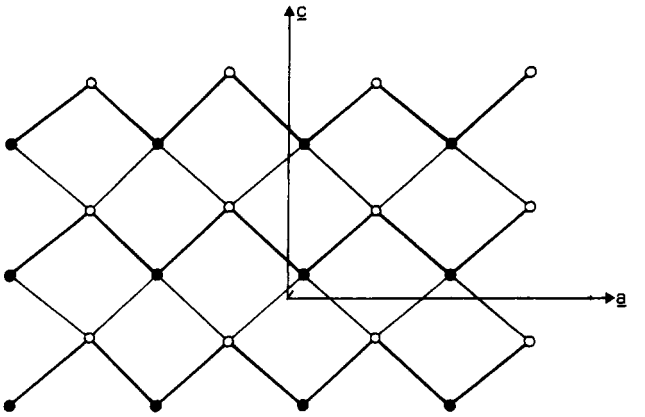

Figure 4. Schematic view of the manganese "lattice" in MnMn-$(EDTA)\cdot 9H_2O$ showing the connections between the chains along the *ac* plane. Filled and open circles correspond to hexacoordinated [Mn1] and heptacoordinated [Mn2] manganese ions, respectively.

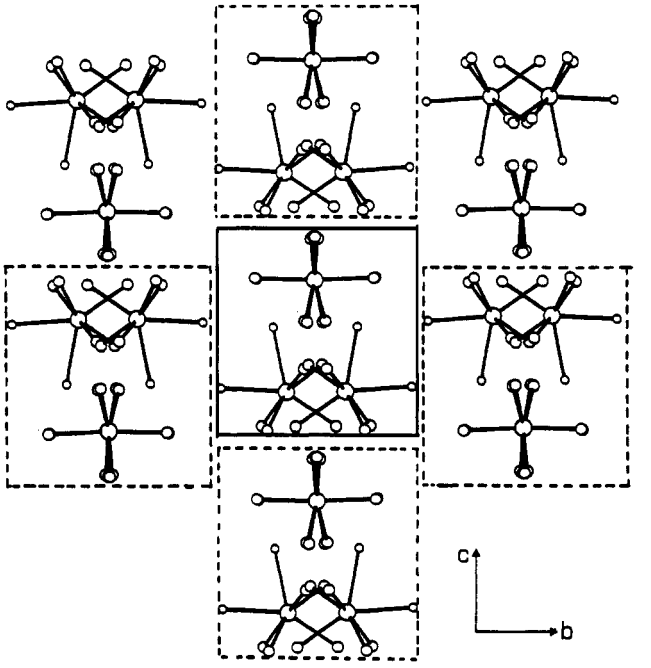

Figure 5. PLUTO view of the chains along the *bc* plane showing that each chain is surrounded by four nearest-neighbor chains.

susceptibility we can proceed no further in our analysis. The change of slope in the in-phase component is a general feature due to the onset of 3D antiferromagnetic ordering. Actually, the theoretical slope below T_c should be infinity.[11] The additional features of the narrow peak in the in-phase component and the small out-of-phase signal in the ordered region indicate the existence of canting; these are the peak due to critical oscillations close to T_c and the out-of-phase signal due to energy absorption arising from domain wall movement of the weakly ferromagnetic phase.

In the present case there is another important feature of the structure that could result in an additional contribution to the ferromagnetism. We notice that the shortest interchain separations involve manganese sites of different natures. Thus, each [Mn1] is surrounded by four nearest-neighbor [Mn2] atoms: two belonging to the same chain at 6.177 and 6.193 Å and the other two belonging to different chains at 6.124 and 6.141 Å (Figures 4 and 5). As a consequence, the (dipolar) antiferromagnetic interactions between adjacent chains will be unable to cancel the (slightly) unequal moments of the two sublattices, giving rise to a net magnetic moment in the ordered state. In this respect, [MnMn]

(10) Bartolomé, J.; Burriel, R. *Physica B+C* **1983**, *115*, 190.

(11) Fisher, M. E. *Philos. Mag.* **1962**, *17*, 1731.

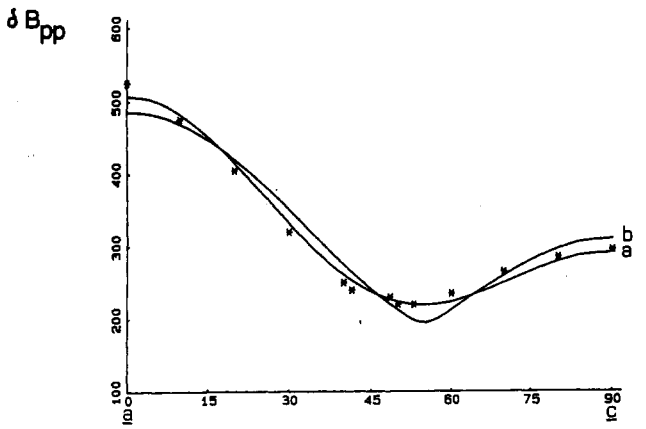

Figure 6. Angular dependence of the ΔB_{pp} (gauss) line width in the *ac* plane at room temperature and Q-band frequency. Full lines correspond to the best fit to expression 3, for $n = 2$ (a) and $n = {}^4/_3$ (b).

may be viewed as a ferrimagnet constructed from ferrimagnetic chains assembled in a ferromagnetic fashion, similar to that found in several bimetallic chain compounds,[12] but with the novelty that this system is homometallic.

The last point deserving discussion concerns the one-dimensional character of this material. One measure of the isolation of the chains is provided by the ratio of J' to J, where J' represents the interchain exchange. In the case of a Heisenberg classical chain, Richards[13] has proposed an expression that relates this ratio to the critical temperature T_c, the intrachain exchange J, and the local spin S. For an orthorhombic lattice in which a chain is weakly coupled to two nearest-neighbor chains by J'_1 and to the other two by J'_2, as is our case (see Figure 4), this expression becomes

$$kT_c = JS(S + 1)[2(J'_1 + J'_2)/J]^{1/2} \quad (2)$$

Using this expression, we obtain $(J'_1 + J'_2)/J = 2.8 \times 10^{-2}$. In the present case, the relevant interchain distances are 6.124 and 8.046 Å. Owing to the dipolar nature of the interchain interaction, a simple r^{-3} dependence of $J'_{1,2}$ upon Mn–Mn separation r allows us to estimate $J'_1/J'_2 \approx 2$ and, finally, $J'_1/J = 2.0 \times 10^{-2}$ and $J'_2/J = 0.8 \times 10^{-2}$. These ratios are 1 order of magnitude larger than those estimated for the bimetallic Heisenberg chains MnNi(EDTA)·6H_2O and MnCu(EDTA)·6H_2O,[5] in agreement with the better isolation of chains in the hexahydrate series, for which the shortest interchain Mn–Mn distance is 7.34 Å.

Single-Crystal EPR Spectra. Suitable EPR single crystals of MnMn(EDTA)·9H_2O show well-developed $\bar{1}0\bar{1}$ and 101 faces, so that the spectra were recorded with rotation around three orthogonal directions X, Y, and Z, with Y parallel to b and with X perpendicular to the 101 face, making an angle of 41.5° with a. The respective direction cosines in the orthorhombic cell are

	a	*b*	*c*
X	0.7489	0	0.6226
Y	0	1	0
Z	−0.6626	0	0.7489

Only one signal centered at $g = 2.0$ is observed for each orientation of the static magnetic field at both X- and Q-band frequencies, showing a practically frequency-independent line width. The low-temperature spectra show a general broadening of the lines without any evidence of *g*-shift effects.

The angular dependence of the line width resembles that of low-dimensional magnetic materials, with a maximum in the peak-to-peak width ($\Delta B_{pp} = 525$ G) along a, the chain direction, and a minimum ($\Delta B_{pp} = 235$ G) at $\theta = 55°$ from a (Figure 6).

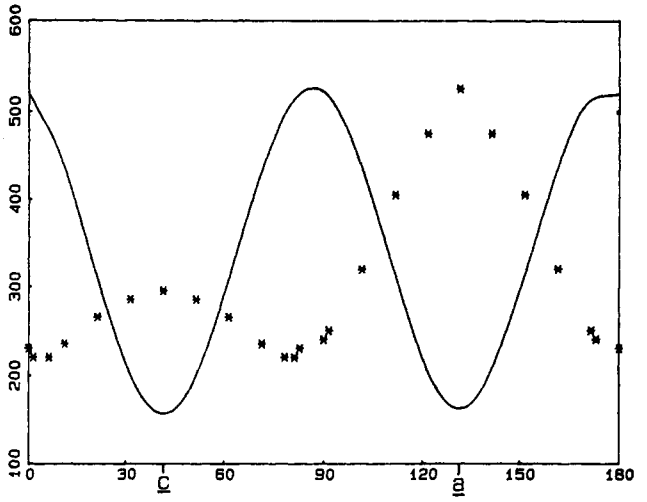

Figure 7. Angular dependence in the *XZ* (*ac*) plane of the experimental line width ΔB_{pp} (gauss) at room temperature and Q-band frequency (*) and of the secular contribution to the dipolar second moment (—) for MnMn(EDTA)·9H_2O.

The line width along b is comparable to that along c. In fact, this behavior can be reproduced with functions of the type

$$\Delta B_{pp} = a + b(3\cos^2\theta - 1)^n \quad (3)$$

with $n = {}^4/_3$, 2, which are typical of one-dimensional linear chains ($n = {}^4/_3$) or two-dimensional ($n = 2$) Heisenberg antiferromagnets.[14-16]

For the analysis of the angular dependence of the line width, we assumed, in a first step, that the dipolar coupling is the responsible for the broadening of the lines. Considering the spins localized on the manganese ions, we attempted to estimate this effect by evaluating the dipolar contribution to the second moment relative to the [Mn]–[Mn] interactions:[17-22]

$$M_2 = (3/4)S(S + 1)\mu_B^2 g^2 \sum_i \sum_j r_{ij}^{-6}\{(3\cos^2\theta_{ij} - 1)^2 + (\sin^4\theta_{ij})\exp[-(1/2)(2\omega_0/\omega_e)^2] + (10\cos^2\theta_{ij}\sin^2\theta_{ij})\exp[-(1/2)(\omega_0/\omega_e)^2]\} \quad (4)$$

where ω_0 and ω_e are the Zeeman and exchange frequencies, respectively, and θ_{ij} and r_{ij} are respectively the angle formed by the static magnetic field with the vector connecting the two paramagnetic interacting centers and the distance between them. In the calculations, the summation over i accounts for eight manganese centers, due to the presence of four nonequivalent sites in the unit cell, the other four being related to them by a translation along c (Figure 4). In low-dimensional materials the first secular term of (4) is expected to dominate over the other two nonsecular terms.[16] As expected on the basis of the low-dimensional character of MnMn(EDTA)·9H_2O, the angular dependence of the total second moment is completely unrelated to the observed line width angular behavior, but also using only the secular component of M_2, it is not possible to reproduce the experimental data (Figure 7).

An angular dependence of the line width of the type $(3\cos^2\theta - 1)^2$ is expected also for bidimensional systems, where θ is now the angle between the direction of the external magnetic field and

(12) Kahn, O. In *Organic and Inorganic Low Dimensional Crystalline Materials*; Delhaes, P., Drillon, M., Eds.; NATO-ASI Series B168; Plenum Press: New York, 1987.
(13) Richards, P. M. *Phys. Rev. B* **1974**, *10*, 4687.
(14) Richards, P. M. *Local Properties at Phase Transitions*; Editrice Compositori: Bologna, Italy, 1975; p 539.
(15) Bartkowsky, R. R.; Hennessy, M. J.; Morosin, B.; Richards, P. M. *Solid State Commun.* **1982**, *11*, 405.
(16) Bencini, A.; Gatteschi, D. *EPR of Exchange Coupled Systems*; Springer-Verlag: Berlin, Heidelberg, 1990.
(17) Kubo, R.; Tomita, K. *J. Phys. Soc. Jpn.* **1954**, *9*, 888.
(18) Drumheller, J. E. *Magn. Reson. Rev.* **1982**, *7*, 123.
(19) Hennessy, M. J.; McElwee, C. D.; Richards, P. M. *Phys. Rev. B* **1973**, *7*, 930.
(20) McGregor, K. T.; Soos, Z. G. *J. Chem. Phys.* **1976**, *64*, 2506.
(21) Van Vleck, J. H. *Phys. Rev.* **1949**, *74*, 1168.
(22) Gatteschi, D.; Guillou, O.; Zanchini, C.; Sessoli, R.; Kahn, O.; Verdaguer, M.; Pei, Y. *Inorg. Chem.* **1989**, *28*, 287.

the perpendicular to the magnetic plane. The structural features of the present compound might suggest some bidimensional character in the *ac* plane (Figure 4); however, no reliable exchange pathways yielding to magnetic bidimensionality can be found in the *bc* plane, perpendicular to the direction exhibiting maximum line width, thus eliminating such a possibility.

Between other possible broadening mechanisms, the single-ion zero-field splitting (ZFS) must be taken into consideration.[16] The second moment for an axial zero-field splitting is given by

$$M_2 = (D^2/10)(2S - 1)(2S + 3)(1 + \cos^2 \theta) \qquad (5)$$

where θ is the angle of the static magnetic field with the unique axis of the zero-field-splitting tensor, **D**. [Mn1] and [Mn2] can have different **D** tensors. Literature data for Mn(II) compounds indicate that D generally does not exceed 0.1 cm^{-1} in distorted octahedral environments, even if several systems appear to have larger values,[23] but similar information is not available for heptacoordinated manganese ions. An estimation of the principal values of **D** in the heptacoordinated site can be obtained from the EPR spectra of Mn(II) doped into the diamagnetic compound MgMg(EDTA)·$9H_2O$. In fact, it has been shown that, in this solid, Mn(II) occupies a heptacoordinated site similar to that found in MnMn(EDTA)·$9H_2O$.[7] A polycrystalline sample containing 1% manganese gives a spectrum that can be simulated reasonably well with values of the ZFS parameters of $D \approx 0.11$–0.13 cm^{-1} and $E/D \approx 0.03$. On the other hand, a similar procedure performed on Mn(II)-doped ZnZn(EDTA)·$6H_2O$ samples allows us to obtain values of $D \approx 5.4 \times 10^{-3}$ cm^{-1} and $E/D \approx 0$ for Mn(II) occupying an octahedral hydrated site. From these D values we can finally evaluate, using expression 5, the contribution of the single-ion ZFS effects on the broadening of the EPR lines in the manganese chain. We notice that the [Mn1] contribution is much smaller than the dipolar one, while for [Mn2] this exceeds the dipolar one, with a ratio of 5:1 for the maximum value of line width. Thus, the experimental angular dependence of the line width could be explained by assuming that the ZFS is directed along *a*, but until independent experimental information is obtained, we cannot speculate further on this point. Although a D value of the order of 0.1 cm^{-1} should lead to some magnetic anisotropy, evidence of *g*-shift effects has been observed down to 4 K. Probably the influence of D on the preferred spin orientations is still too slight at this temperature.

Finally, with regard to the line shape, an analysis of the spectra with the field along the three crystallographic axes, and at $\theta = 55°$ from *a*, is reported in Figure 8. We notice that the curve is Lorentzian at the magic angle ($\theta = 55°$ from *a*), nearly Lorentzian along *a*, and intermediate between Lorentzian and Gaussian along *b* and *c*. For an ideal one-dimensional system, the line shape can be described by a Lorentzian curve at the magic angle and by the Fourier transform of $\exp(-t^{3/2})$ along the chain (see Figure 8). The fact that the line shape is nearly Lorentzian along *a* is in agreement with the presence of nonnegligible interchain interactions of the order of magnitude estimated from magnetic data ($J'/J \approx 10^{-2}$).

(23) Carlin, R. L. *Magnetochemistry*; Springer-Verlag: Berlin, Heidelberg, 1986.

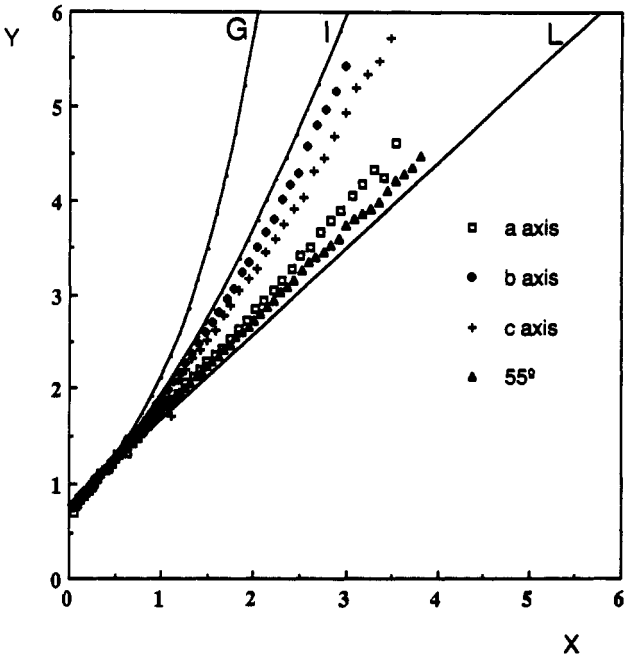

Figure 8. Line shape data. Plot of $[(I'_m/I')(B - B_0)(^1/_2\Delta B_{pp})]^{1/2}$ versus $[(B - B_0)/\Delta B_{pp}]^{1/2}$ for a Lorentzian fit (L), a Gaussian fit (G), and a Fourier transform of $\exp(t^{-3/2})$ and for the observed line shapes at the indicated directions.

Conclusion

We have discussed in this paper the magnetic and EPR properties of the two-sublattice chain MnMn(EDTA)·$9H_2O$, which is formed by alternating hexa- and heptacoordinated metal sites. The interplay between these two techniques has allowed us to obtain a satisfactory characterization of this system. Thus, the magnetic susceptibility data have provided information on intrachain ($J = -0.5$ cm^{-1}) and interchain interactions ($J'/J \approx 10^{-2}$) but appeared to be insensitive to the single-ion zero-field-splitting effects. In turn, this effect has been shown to be quite prominent in the broadening of the EPR lines. In the chains reported so far, the angular dependence of the line widths was discussed in relation to dipolar interactions between the paramagnetic centers.[22] In our case, the large intermetallic separations, together with the magnitude of the zero-field splitting of heptacoordinated manganese ($D \approx 0.11$–0.13 cm^{-1}), results in a broadening of the line controlled by single-ion zero-field-splitting effects.

Acknowledgment. This work was supported by the Comisiõn Interministerial de Ciencia y Tecnologia (Grants PB 85-106 and MAT 89-177), by the Institució Valenciana d'Estudis i Investigació, and by an Italo-Spanish Integrated Action (No. 41). J.J.B.-A. and C.J.G.-G. acknowledge the Ministerio de Educaciõn y Ciencia for a fellowship. E.C. thanks the Generalitat Valenciana for a travel grant. The financial support of the Italian Ministry of Public Education and the CNR is gratefully acknowledged. We are deeply grateful to R. L. Carlin for allowing us to perform the ac magnetic measurements on his apparatus.